RSC Advances

PAPER

View Article Online
View Journal | View Issue

Check for updates

Cite this: *RSC Adv.*, 2025, **15**, 21785

Advanced electrochemical treatment of tetracycline-contaminated water using Pt/Ti electrodes†

Natalia. A. Ivantsova,[a] Eugene N. Kuzin,[a] Vitaly V. Kuznetsov,[b] Elena A. Filatova,[a] Andrey V. Pirogov,[c] Yury V. Timchenko,[c] Frederic Poineau, *[d] Konstantin E. German,[b] Yulia M. Averina[a] and Artem V. Kolesnikov[a]

The electrochemical mineralization of tetracycline in chloride aqueous solutions using Pt/Ti anodes has been investigated. The mineralization process, oxidation efficiencies and oxidation products were characterized by UV-visible spectroscopy and HPLC-MS. Tetracycline oxidation efficiencies are 97 ± 2% in 0.64 wt% HCl and 85 ± 3% in 0.64 wt% NaCl within 15 minutes of electrolysis. UV-visible spectroscopy confirmed the degradation of the antibiotic's π-conjugated electron system and allowed the identification of active species (*i.e.*, hydrogen peroxide and dissolved chlorine) that can potentially degrade tetracycline. The formation of these active species is due to the high positive potential of the Pt/Ti anode during electrolysis. HPLC-MS studies show the intensity of the tetracycline peak to gradually decrease during electrolysis, indicating its oxidation. Peaks corresponding to oxidation intermediates with a molecular weight above 70 were not detected, which indicates the absence of oxidation products with higher molecular mass. During electrochemical oxidation of tetracycline, small amounts of formaldehyde are formed, but its concentration can be brought to an acceptable level by diluting the solution. In negative mode, chlorate ions were detected in the NaCl solutions, which are likely formed from the stepwise oxidation of chloride ions; however, this phenomenon is not observed in HCl solutions.

Received 15th April 2025
Accepted 17th June 2025

DOI: 10.1039/d5ra02632f

rsc.li/rsc-advances

Open Access Article. Published on 25 June 2025. Downloaded on 12/7/2025 12:10:05 AM.
This article is licensed under a Creative Commons Attribution-NonCommercial 3.0 Unported Licence.

Introduction

The extensive use of antibiotics in agriculture and healthcare industries has contributed to the emergence of antibiotic-resistant microorganisms, presenting a growing threat to global health.[1–4] One of these antibiotics is tetracycline, a broad-spectrum agent that exhibits activity against a wide range of Gram-positive and Gram-negative bacteria.[5]

The use of antibiotics during the treatment of SARS-CoV-2 has led to the significant presence of unmetabolized species in wastewater.[6,7] These antibiotics enter the sewage system, and elevated levels have been detected in surface and groundwater.[8–12] Antibiotics are widely used in livestock and poultry farming for preventive and supportive treatments. Waste containing antibiotics is often disposed-of improperly, leaching into water.[13–18]

Studies on antibiotic removal from wastewater have revealed that conventional methods using hydrogen peroxide, ozone, and hypochlorite ions have low mineralization efficiency.[19–22] Advanced oxidation processes (AOPs), which generate highly reactive radicals, are considered the most promising methods for the mineralization of antibiotics.[19,22–25] The use of AOPs faces challenges such as complex system designs, high reagent consumption and operational costs.[26–29] An alternative approach to AOPs is the oxidation using ferrates, which offers efficient removal at a relatively low cost.[30–33] AOPs are effective for antibiotics at concentrations below 2 mg L^{-1} but require initial treatment for higher concentrations.[20,22–25] Supercritical water oxidation, another potential treatment, is hindered by its high operational costs and complexity.[27,34,35] Electro-oxidation provides a simple and cost-effective method for treating highly concentrated pollutants.[36–39]

Concerning tetracycline, AOPs can achieve up to 99% mineralization for concentrations between 0.1 and 1.0 mg L^{-1} but treatments for higher concentrations are lacking. Electro-oxidation has shown promise for tetracycline removal, with residual pollutants easily removed by subsequent AOPs.[40,41] Several studies have explored electro-oxidation of tetracycline, employing various anode materials such as Pb/PbO_2, Nb/BDD,

[a]*D. I. Mendeleev University of Chemical Technology of Russia, Moscow, 125047, Russian Federation*
[b]*A. N. Frumkin Institute of Physical Chemistry and Electrochemistry, Russian Academy of Sciences, 119071 Moscow, Russian Federation*
[c]*M. V. Lomonosov Moscow State University, 119991 Moscow, Russian Federation*
[d]*Department of Chemistry and Biochemistry, University of Nevada Las Vegas, 4505 Maryland Parkway, Las Vegas, NV 89154, USA. E-mail: poineauf@unlv.nevada.edu*
† Electronic supplementary information (ESI) available: See DOI: https://doi.org/10.1039/d5ra02632f

Open Access Article. Published on 25 June 2025. Downloaded on 12/7/2025 12:10:05 AM. This article is licensed under a Creative Commons Attribution-NonCommercial 3.0 Unported Licence.

and Ti/RuO_2–IrO_2.[42–48] So far, complete mineralization of tetracycline has not been achieved, and the nature of the oxidation products remains underexplored. The presence of chloride ions during electrolysis generates active species that may enhance oxidation.[47]

Here, we explore the electrochemical oxidation of tetracycline using Pt/Ti anodes in aqueous chloride media, assess the degree of mineralization, and identify the oxidation products.

Experimental section

Materials

Tetracycline (Tyumen Chemical-Pharmaceutical Plant), HCl (12 M, reagent grade, Reachim), NaCl (reagent grade, Reachim) and deionized water (R > 18 MΩ cm, TOC < 3 ppb) were used. The 8 wt% HCl solution was prepared by diluting 12 M HCl.

Electrochemical methods

Electro-oxidation experiments were conducted under galvanostatic conditions (I = 0.1–0.4 A) using a DAZHENG PS-305D PC Power Supply. The anolyte (120 mL) contained tetracycline dissolved in HCl or NaCl solution, and the catholyte (40 mL) contained all components except tetracycline. Pt/Ti anodes (YUNCH, China),[47] (S_{geom} = 10 cm^2) and Ti cathodes were used. For Pt/Ti anodes, the manufacturer indicates[48] a platinum layer thickness of 0.5–10 μm (platinum loading of 1–20 mg cm^{-2}) and that thermal decomposition of platinum salts on titanium substrate was used to prepare the electrode. Our ICP-MS analysis, performed after dissolution of the active layer of anode in *aqua regia*, showed an average platinum loading of ~5 mg cm^{-2}.

The choice of Pt/Ti anodes for indirect tetracycline electrooxidation is due to their commercial availability. Moreover, efficient generation of active oxygen and chlorine containing species is only possible at high anodic potentials. Oxygen evolution begins at E > 1.7 V (RHE) on Pt/Ti electrodes and dissociative adsorption of organic molecules further causes a positive shift in the potential.

Ti/PbO_2 electrodes are also characterized by positive oxygen evolution potentials. However, Pb(II) ions are toxic, and their formation, which can occur during current interruptions, is from an environmental and health point of view unsustainable. The most positive potentials can be reached using boron-doped diamond (BDD) anodes; however, this material is scarce and has not yet been commercialized.

The Ti_4O_7 anodes, exhibit strong oxidation performance for the degradation tetracycline.[47,49,50] These electrodes exhibit good conductivity, but they can undergo degradation over time accompanied by an increase in the resistance of the interphase boundary.[51] This drawback can be addressed using complex preparation methods, *e.g.* deposition of an Ir@IrO_x layer.

Polarization measurements were conducted in a standard three-electrode cell. The working electrode potential was referenced against a saturated Ag/AgCl electrode. All potentials were calculated to a reversible hydrogen electrode (RHE) in the same solution. A digital potentiostat IPC-MS (Volta) was used for measurements under potentiodynamic conditions. Solutions were bubbled with argon gas for 30 minutes prior experiments.

Microscopic and diffraction methods

Surface morphology was analyzed using a Thermo Fisher Scientific Quattro S SEM, equipped with secondary electron, backscattered electron, and energy-dispersive X-ray detectors (Bruker SDD). SEM images were recorded under high vacuum conditions with currents ranging from 87 pA to 200 nA and accelerating voltages between 2 kV and 30 kV. The phase composition was examined by powder X-ray diffraction using a Bruker D8 ADVANCE diffractometer with Cu Kα radiation (λ = 1.5406 Å).

Analytical methods

HPLC-MS analysis was performed using a Dionex Ultimate 3000 chromatograph (Thermo Fisher Scientific) coupled with an Orbitrap Elite Hybrid ion trap mass spectrometer (Thermo Fisher Scientific). Chromatographic separation was conducted on a Shim-pack GIST-HP C18-Aq column (150 × 3 mm, 3 μm) with a mobile phase consisting of 0.1% formic acid in deionized water and 0.1% formic acid in isopropyl alcohol at a flow rate of 0.3 mL min^{-1}. The analysis time was 30 minutes, and mass spectra were obtained in both positive and negative modes over the 103–1500 m/z range. Samples (1 mL) were taken at different electrolysis times, mixed with NaOH (200 mL, 0.2 M), and centrifuged.

Chemical oxygen demand (COD) was measured using a photometric method. Potassium dichromate and sulfuric acid were added to the sample, and silver sulfate was used to remove chloride ions. After heating at 150 °C for 2 hours, absorbance was measured at 400 nm (COD 10–160 mgO_2 L^{-1}) or 600 nm (COD 160–800 mg_{O_2} L^{-1}).

UV-visible spectra were recorded using a SF-2000 digital spectrophotometer. The concentration of tetracycline was monitored using a photoelectric colorimeter (CPC-3) at 360 nm. The absorption spectrum of the tetracycline displays two distinct bands at 276 and 360 nm (Fig. S1†). Formaldehyde was identified using a colorimetric method.[52]

Chlorate ions were detected by ion-exchange chromatography using ion chromatograph dionex ISC-3000 in reagent-free suppressor IC mode. Gradient (NaOH) elution was used.

Characterization of the electrodes

Electrochemical treatment of aqueous tetracycline solutions was performed using Pt/Ti anodes. The cyclic voltammogram (Fig. S2†) at the Pt/Ti anode reveals hydrogen, double-layer, and oxygen regions typical for platinum electrodes. The hydrogen region is asymmetric, indicating a hydrogen spillover effect. Platinum oxide formation begins around 0.8 V, a behavior characteristic of platinum electrodes.

The morphology of Pt/Ti anodes was analyzed by SEM. The surface of Pt/Ti electrodes (Fig. S3†) contains platinum clusters composed of nanoparticles. During electrolysis, these platinum nanoparticles serve as active sites for the formation of reactive chlorine and oxygen species. The SEM images were taken after

© 2025 The Author(s). Published by the Royal Society of Chemistry

Open Access Article. Published on 25 June 2025. Downloaded on 12/7/2025 12:10:05 AM.
This article is licensed under a Creative Commons Attribution-NonCommercial 3.0 Unported Licence.

1000 hours of electrolysis, demonstrating the nanoparticles to remain stable under these conditions. The powder X-ray diffraction pattern of the Pt/Ti electrodes (Fig. S4†) shows reflections corresponding to the platinum phase. Using the Scherrer equation, the average size of the platinum nanoparticles was estimated to be ~20 nm.

Carbon monoxide monolayer desorption was performed to determine the electrochemically active surface area (EASA) of the electrode (Fig. S5†),[53,54] a coefficient of 0.42 mC cm^{-2} was used for the calculation. The potential region for CO desorption and the shape of the desorption peak are characteristic of platinum catalysts. The EASA (25.0 cm^2) remains constant after electrolysis under oxygen evolution, highlighting the stability of the electrode material.

Results and discussion

Using tetracycline in its commercial form simulates practical conditions, as both active ingredients and auxiliary agents are present in wastewater. During electrolysis, chlorine and oxygen species may oxidize the auxiliary agents instead of tetracycline, so studying tetracycline in its commercial form is essential before applying wastewater treatment methods.

A tetracycline-LekT tablet containing tetracycline hydrochloride (~1 g) was crushed in an agate mortar, weighed, and dissolved in 20 mL of either 8 wt% HCl or 8 wt% NaCl. The solution was then diluted to 250 mL with DI water. Chloride-containing media were found to produce the best results for tetracycline oxidation.[47,55] Electro-oxidation was performed in 0.64 wt% solutions of HCl (initial pH = 0.8) or sodium chloride (initial pH ~6.0).

In 0.64 wt% HCl, anodic processes occur above 1.3 V (Fig. 1a), primarily involving oxygen and chlorine evolution. The introduction of tetracycline in the solution significantly inhibits these anodic reactions. It is likely that tetracycline molecules adsorb *via* O atoms onto the platinum surface inhibits anodic processes. A similar phenomenon, where the oxidation of Br^- ions is inhibited by small amounts of phenol, has been reported.[56]

The shift toward positive potentials promotes the formation of active oxygen and chlorine species, which may contribute to the complete mineralization of tetracycline. A similar effect was observed in NaCl solutions (Fig. 2b). Due to oxygen evolution, the near-anodic layer becomes acidic and thus anodic processes in both HCl and NaCl solutions occur at similar potentials.

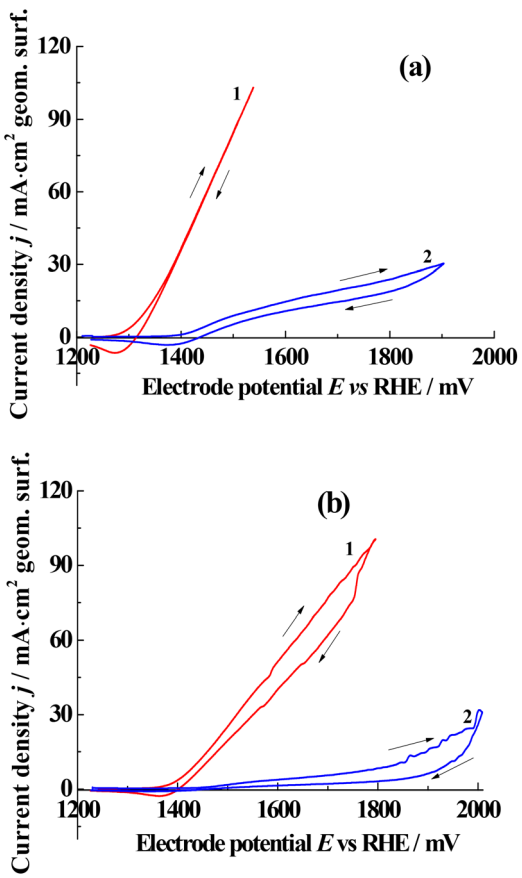

Fig. 1 Potentiodynamic (5 mV s^{-1}) polarization curves in 0.64 wt% HCl (a) and 0.64 wt% NaCl (b) solutions. 1 – blank solution of HCl (red curve) and NaCl (blue curve), 2 – tetracycline (1.09 mg L^{-1}).

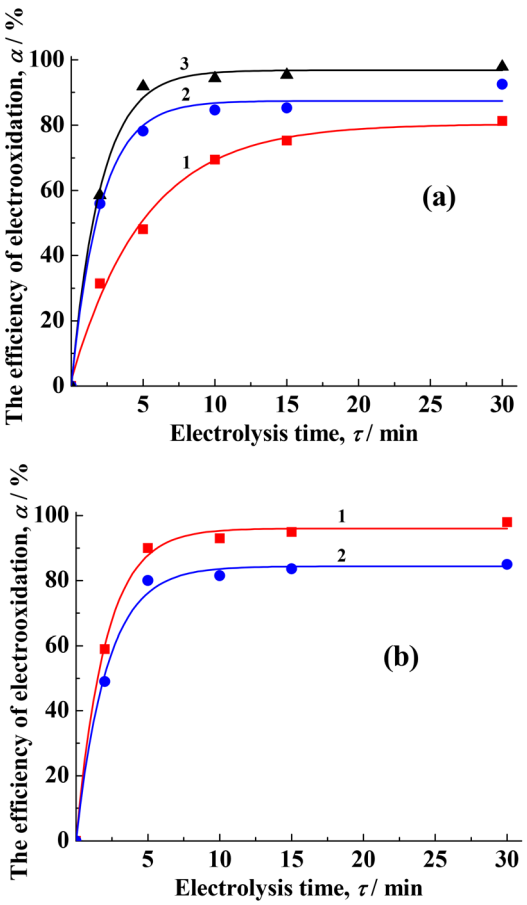

Fig. 2 (a) Tetracycline electrooxidation efficiency as a function of electrolysis time for different initial concentrations (c_{in}, mg L^{-1}) in 0.64 wt% HCl: 1 = 80 (in red), 2 = 40 (in blue), 3 = 15 (in black). (b) Oxidation of tetracycline (c_{in} = 20 mg L^{-1}) in 0.64 wt% HCl (1, in red) and 0.64 wt% NaCl (2, in blue) solutions. I = 0.4 A, j = 0.04 A cm^{-2}.

Open Access Article. Published on 25 June 2025. Downloaded on 12/7/2025 12:10:05 AM.
This article is licensed under a Creative Commons Attribution-NonCommercial 3.0 Unported Licence.

The electro-oxidation of tetracycline in HCl solution is highly efficient. When the initial concentration of tetracycline is 15 mg L^{-1}, the oxidation yield reaches 97 ± 2% within 15 minutes of electrolysis (Fig. 2a). At higher concentrations of tetracycline (80 mg L^{-1}), complete oxidation is not achieved in 30 minutes (yield: 81 ± 3%). The energy consumption for tetracycline removal calculated from the values of current, cell voltage and duration of electrolysis, was estimated to be ~0.3 kW h per gram of tetracycline in acidic media.

The efficiency of tetracycline electro-oxidation is slightly dependent on solution acidity, showing oxidation rate of (97 ± 2%) in 0.64 wt% HCl and (85 ± 3%) in 0.64 wt% NaCl (Fig. 2b). These values are comparable to that reported for oxytetracycline,[47] where 96% of oxytetracycline was oxidized after 3 hours of electrolysis using Pt/Ti anodes in 40 mM NaCl solution. This is likely due to the acidification of the near-anode region caused by oxygen evolution, the primary anodic process in both solutions. The pH of the anolyte in NaCl decreases to 3.0 within 3 minutes of electrolysis, reaching 2.5 after 10 minutes and remaining stable. Meanwhile, the pH of the catholyte solution increases to 12.5.

The degradation of tetracycline was studied by UV-visible spectroscopy during the electrochemical treatment. Bands at 276 and 360 nm (Fig. 3) of the initial solution are due to π-conjugated electron system (C=C and C=O bonds). These bands disappear after 10 minutes of electrolysis, which indicates the degradation of tetracycline and the absence of accumulation in significant quantities of substances containing conjugated π-bonds, primarily quinones.[49] It is proposed that active chlorine and oxygen species generated at the anode play an active role in the degradation process.

UV-visible measurements support this hypothesis, as the spectra of tetracycline in 0.64 wt% HCl during electrolysis (Fig. 4) show the appearance of bands at 223 nm and 350 nm respectively consistent with the formation of hydrogen peroxide[57,58] and dissolved chlorine.[59] It is likely that active species, *e.g.* ·Cl and ·OH, generated during electrolysis degrade the tetracycline molecules. Theoretically, the contribution of free radicals could be distinguished by radical quenching experiments. However, radical scavengers undergo dissociative chemosorption on platinum anodes,[60,61] which inhibits electrode reaction and affects the experiment results.

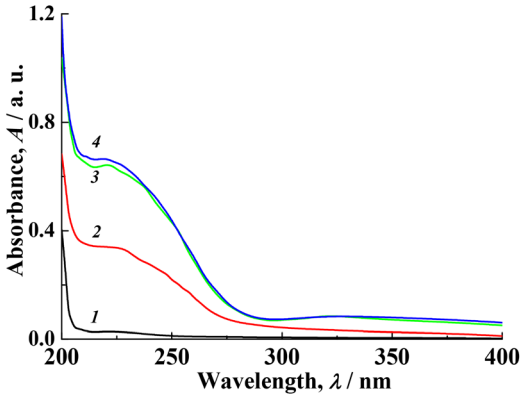

Fig. 4 UV-visible spectra of a solution of HCl (0.64 wt%) during electrolysis (Pt/Ti anode, I = 0.2 A, j = 0.02 A cm^{-2}). Time of electrolysis (min): 1 = 0, 2 = 5, 3 = 10, 4 = 15.

XPS analysis (Fig. S6†) of the Pt/Ti electrode after tetracycline oxidation, showed the presence of platinum metal, oxygen, chlorine, and carbon. The carbon content decreases after ion etching at a depth of 5 nm and the C1 peak suggests the presence of carbon-containing contaminants.

Tetracycline oxidation efficiency is comparable in both acidic and neutral solutions. Due to the oxygen evolution, the near-electrode region is more acidic than the bulk solution. Since tetracycline degradation occurs in this region, where active oxygen and chlorine species are concentrated, the oxidation rate in both acidic (pH = 2–3) and neutral (pH = 5–6) solutions are comparable (Fig. 5). Initially, the oxidation rate differs by a factor of 1.3 as the near-electrode acidity is still adjusting. After 10 minutes of electrolysis, the residual

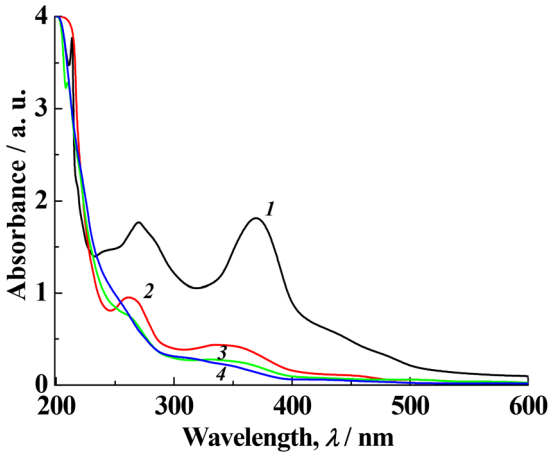

Fig. 3 UV-visible spectrum of tetracycline in 0.64 wt% HCl as a function of electrolysis time. Initial concentration of tetracycline c_{in} = 80 mg L^{-1}, j = 0.02 A cm^{-2}, I = 0.2 A. Time of electrolysis (min): 1 = 0 (in black), 2 = 5 (in red), 3 = 10 (in green), 4 = 20 (in blue).

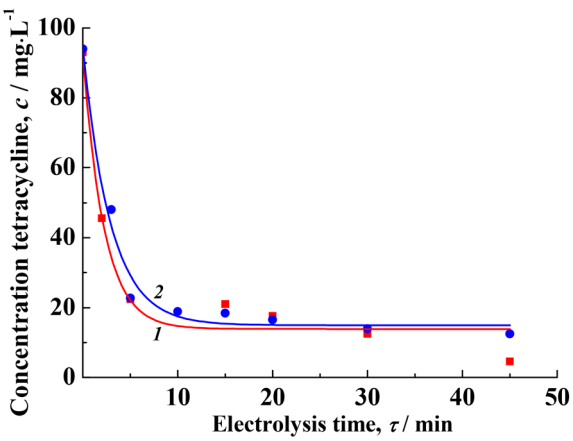

Fig. 5 Tetracycline concentration as a function of electrolysis time in (1) 0.64 wt% HCl (in blue) and (2) NaCl (in red) solutions. I = 0.4 A, j = 0.04 A cm^{-2}.

© 2025 The Author(s). Published by the Royal Society of Chemistry

Open Access Article. Published on 25 June 2025. Downloaded on 12/7/2025 12:10:05 AM.
This article is licensed under a Creative Commons Attribution-NonCommercial 3.0 Unported Licence.

Table 1 Chemical oxygen demand values during the electrolysis of 0.64 wt% NaCl containing 80 mg L^{-1} tetracycline. $I = 0.4$ A, $j = 0.04$ A cm^{-2} after 15 min and 30 min. $I = 0.2$ A, $j = 0.02$ A cm^{-2}

Time (min)	0 (Initial)	15	30
COD (mg_{O_2} L^{-1})	313	285	91

tetracycline concentrations in both solutions approach values (17–20 mg L^{-1}, Fig. 5) corresponding to its removal by 80–85%.

Chemical oxygen demand value indicates the amount of oxygen needed for oxidation of organic substances in an aqueous solution. Its sharp decrease in the first 30 minutes of electrolysis (Table 1) indicates a high degree of tetracycline mineralization to products, which cannot be oxidized by dichromate ions. Value of 91 mgO_2 L^{-1} may be due to the presence of residual organic metabolites after electrochemical treatment; these metabolites were identified by HPLC/MS (*vide infra*).

The degradation of tetracycline is a complex process and the formation of toxic intermediates during electrochemical treatment is problematic. Possible intermediates (*e.g.* quinones) of tetracycline oxidation at Ti/Ti_4O_7 anodes were reported[49] and their toxicity was assessed using a standard water test method based on the bioluminescence of *Vibrio fischeri* bacteria.

To monitor tetracycline oxidation, mass spectra in both positive and negative ions were recorded in NaCl solution. Results (Fig. 6 and Table 2) show that tetracycline (retention time of 11.64 minutes) was detected in the mass spectra of the initial solutions, in both positive and negative modes.

In positive mode, the mass spectrum shows a peak at m/z = 445.16 corresponding to the protonated form of tetracycline (Fig. 6)[62] while in negative mode, tetracycline, in its deprotonated form appears at $m/z = 443.14$, a pre-peak at 10.94 minutes is likely attributed to a tetracycline structural isomer, doxycycline,[63] as its molecular peak matches at $m/z = 445.16$ (positive mode).

The intensity of the tetracycline peak gradually decreases during electrolysis, indicating its oxidation. Peaks corresponding to possible oxidation intermediates (*e.g.* quinones)[49] were not detected (Fig. 6), suggesting that contaminants with a molecular weight above 70 were not produced during oxidation. In negative mode, chlorate ions (ClO_3^-, m/z = 83, 85, intensity ratio 3 : 1) were detected and likely formed during the stepwise oxidation of chloride.[50] By analogy with sodium acetate cations (*i.e.*, $Na^+(CH_3COO{-}Na^+)_n$) the formula $M^+(HCOO{-}M^+)_n$ (M = Na, Ca) is proposed.[64]

The formation of ClO_3^- ions in neutral NaCl solutions raises toxicity concerns. After electrolysis in 0.5 M NaCl, a relatively high chlorates concentration (~28 ppm) was measured by ion-exchange chromatography. The formation of chlorate ions does not occur in acid solutions (Fig. S7†) due to their reaction with chloride:

$$5Cl^- + ClO_3^- + 6H^+ \rightarrow 3Cl_2 + 3H_2O \quad (1)$$

Therefore, electrolysis in HCl solutions prevents the formation of chlorates.

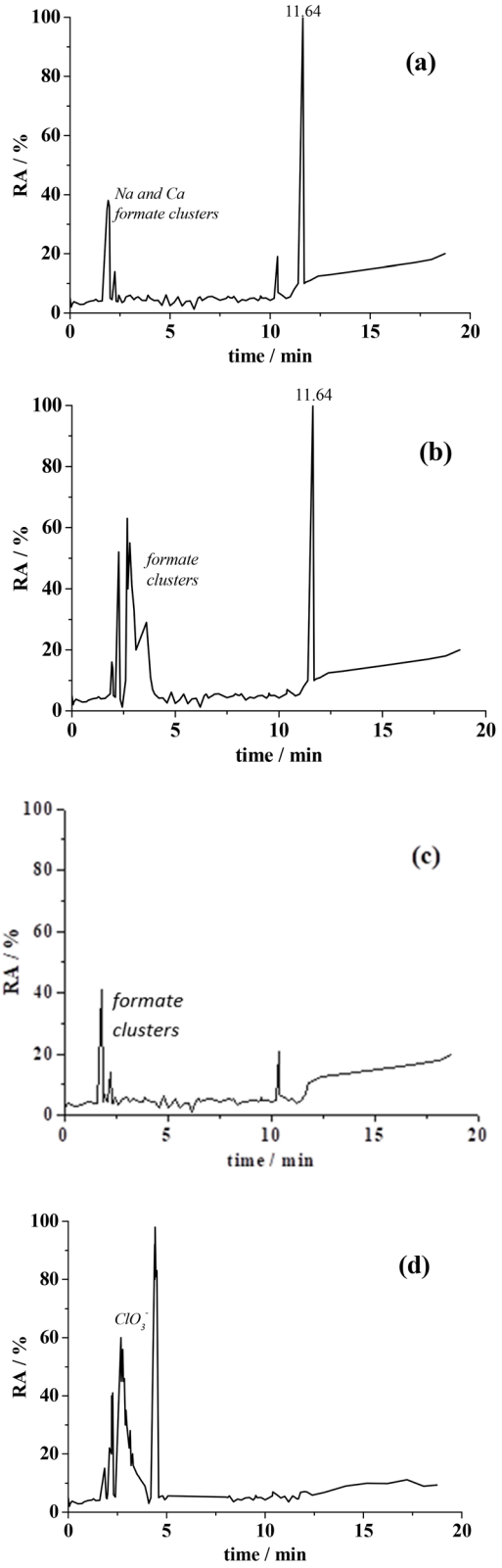

Fig. 6 Monitoring of tetracycline (10 mg L^{-1}) oxidation ($I = 0.2$ A, j = 0.02 A cm^{-2}) in 0.64 wt% NaCl by HPLC-MS. Chromatograms of initial solution in positive (a) and negative mode (b); chromatograms after 30 min of electrochemical treatment in positive (c) and negative mode (d).

Open Access Article. Published on 25 June 2025. Downloaded on 12/7/2025 12:10:05 AM. This article is licensed under a Creative Commons Attribution-NonCommercial 3.0 Unported Licence.

Table 2 Retention time, m/z, intensity and attribution of species found by HPLC-MS during the electroxidation of tetracycline (10 mg L^{-1}) in 0.64 wt% NaCl. $I = 0.2$ A, $j = 0.02$ A cm^{-2}

Mode	Retention time (min)	m/z	Intensity (%)	Species
Negative	1.90–3.00	515, 433 and others	80	Clusters of sodium and calcium cations with formate anions[64]
Negative	4.37	83, 85	15	ClO_3^-
Negative	11.65	443.16	<5	Tetracycline
Negative	10.94	443.16	<1	Doxycycline
Positive	1.94–2.25	515 and others	90	Clusters of sodium and calcium cations with formate anions[64]
Positive	11.64	445.16	10	Tetracycline
Positive	10.94	445.16	<1	Doxycycline

The concentration of formaldehyde determined after the oxidation (30 min) of tetracycline (10 mg L^{-1}) for two current value (0.43(2) mg L^{-1} at 0.2 A and 0.71(3) mg L^{-1} at 0.5 A) is above the maximum allowable concentration for water bodies used in fisheries (0.25 mg L^{-1} in the Russian Federation, 0.05 mg L^{-1} in the United Kingdom[65] and 0.11 mg L^{-1} in the United States[66]). The authors note that reaching drinking water concentration standards is unnecessary, as the water will be discharged into the sewer system, where it will be further diluted. Formaldehyde levels could be reduced to regulatory values using sorption technologies such as adsorption on kaolin and bentonite.[67]

Conclusions

In summary, the electrochemical mineralization of aqueous chloride solutions containing high concentrations of tetracycline was successfully achieved using Pt/Ti anodes. The efficiency values found for the electro-oxidation of tetracycline solutions (>85%) is comparable to other method (*e.g.* 95% for photo-oxidation).[68] Our studies show that the efficiency of commercial Pt/Ti anodes for tetracycline oxidation is comparable with Ti_4O_7 (~95%) and comparable to Ti/RuO_2–IrO_2@Pt anodes (~90%). The adsorption of tetracycline molecules, and their fragments, on the platinum surface shifts the anode potential to more positive values, facilitating the formation of active oxygen and chlorine species. These species interact with tetracycline, leading to the breakdown of its π-conjugated electronic system. In the presence of chloride ions, tetracycline removal is nearly identical in both acidic and neutral solutions due to the acidification of the anolyte from the oxygen evolution reaction. HPLC-MS analysis of tetracycline oxidation showed that organic intermediates do not accumulate significantly during electrolysis. Chlorate ions, doxycycline and clusters of sodium and calcium cations with formate anions were detected and likely formed during the stepwise oxidation process. One concern about the method is the formation of formaldehyde with concentration above regulatory values. Current work focus on reducing these values using sorption technologies and results will be reported in due course.

Data availability

The data supporting this article have been included as part of the ESI.†

Author contributions

N. A. I. – experimental work. E. N. K. – experimental work, methodology. V. V. K. – methodology, writing. E. A. F. – experimental work, writing. A. V. P. – chromatograph mass spectrometry, identification of metabolites. Y. V. T. – chromatograph mass spectrometry, identification of metabolites, analytical experiments. F. P. – writing – review & editing. K. E. G. – methodology, evaluation of experimental results. Y. M. A. – experimental, financial support. A. V. K. – material support for experiments.

Conflicts of interest

There are no conflicts to declare.

Acknowledgements

The work was supported by the Ministry of Science and Higher Education RF.

References

1 E. H. Adator, C. Narvaez-Bravo, R. Zaheer, S. R. Cook, L. Tymensen, S. J. Hannon, C. W. Booker, D. Church, R. R. Read and T. A. McAllister, A One Health Comparative Assessment of Antimicrobial Resistance in Generic and Extended-Spectrum Cephalosporin-Resistant Escherichia coli from Beef Production, Sewage and Clinical Settings, *Microorganisms*, 2020, **8**, 885–906.
2 C. Li, Y. Xu and W. Song, Pollution Characteristics and Risk Assessment of Typical Antibiotics and Persistent Organic Pollutants in Reservoir Water Sources, *Water*, 2023, **15**, 259–275.
3 P. Y. Hong, N. Al-Jassim, M. I. Ansari and R. I. Mackie, Environmental and Public Health Implications of Water Reuse: Antibiotics, Antibiotic Resistant Bacteria, and Antibiotic Resistance Genes, *Antibiotics*, 2013, **2**, 367–399.
4 N. Skandalis, M. Maeusli, D. Papafotis, S. Miller, B. Lee, L. Theologidis and B. Luna, Environmental Spread of Antibiotic Resistance, *Antibiotics*, 2021, **10**, 640–653.
5 I. Chopra and M. Roberts, Tetracycline Antibiotics: Mode of Action, Applications, Molecular Biology, and Epidemiology

© 2025 The Author(s). Published by the Royal Society of Chemistry

Open Access Article. Published on 25 June 2025. Downloaded on 12/7/2025 12:10:05 AM. This article is licensed under a Creative Commons Attribution-NonCommercial 3.0 Unported Licence.

of Bacterial Resistance, *Microbiol. Mol. Biol. Rev.*, 2001, **65**, 232–260.

6 H. Hekmat, A. Rasooli, Z. Siami, K. A. Rutajengwa, Z. Vahabi and F. A. Mirzadeh, A Review of Antibiotic Efficacy in COVID-19 Control, *J. Immunol. Res.*, 2023, **6**, 6687437.

7 S. Kaushik, V. K. Srivastava and B. Mishra, Editorial: Impact of SARS-CoV-2 on Antibiotic Resistance: Evolution of Treatment and Control Strategies, *Front. mol. Biosci.*, 2023, **10**, 1238479.

8 P. Wang, Y.-L. He and Ch.-H. Huang, Reactions of tetracycline antibiotics with chlorine dioxide and free chlorine, *Water Res.*, 2011, **45**, 1838–1846.

9 Z. Maghsodian, A. M. Sanati, T. Mashifana, M. Sillanpää, S. Feng, T. Nhat and B. Ramavandi, Occurrence and Distribution of Antibiotics in the Water, Sediment, and Biota of Freshwater and Marine Environments: a review, *Antibiotics*, 2022, **11**, 1461–1483.

10 H. A. Younes, H. M. Mahmoud, M. M. Abdelrahman and H. F. Nassar, Seasonal occurrence, removal efficiency and associated ecological risk assessment of three antibiotics in a municipal wastewater treatment plant in Egypt, *Environ. Nanotechnol.*, 2019, **12**, 100239.

11 A. Pereira, L. J. G. Silva, C. S. M. Laranjeiro, L. M. Meisel, C. M. Lino and A. Pena, Human pharmaceuticals in Portuguese rivers: The impact of water scarcity in the environmental risk, *Sci. Total Environ.*, 2017, **609**, 1182–1191.

12 M. Pan and L. M. Chu, Occurrence of antibiotics and antibiotic resistance genes in soils from wastewater irrigation areas in the Pearl River Delta region, southern China, *Sci. Total Environ.*, 2018, **624**, 145–152.

13 C. Manyi-Loh, S. Mamphweli, E. Meyer and A. Okoh, Antibiotic Use in Agriculture and Its Consequential Resistance in Environmental Sources: Potential Public Health Implications, *Molecules*, 2018, **23**, 795–842.

14 A. Mann, K. Nehra, J. S. Rana and T. Dahiya, Antibiotic resistance in agriculture: Perspectives on upcoming strategies to overcome upsurge in resistance, *Curr. Res. Microb. Sci.*, 2021, **2**, 100030.

15 S. M. Zainab, M. Junaid, N. Xu and R. N. Malik, Antibiotics and antibiotic resistant genes (ARGs) in groundwater: A global review on dissemination, sources, interactions, environmental and human health risks, *Water Res.*, 2020, **187**, 116455.

16 R. Zhang, S. Yang, Y. An, Y. Wang, Y. Lei and L. Song, Antibiotics and antibiotic resistance genes in landfills: a review, *Sci. Total Environ.*, 2022, **806**, 150647.

17 A. Tiwari, P. Kurittu, A. I. Al-Mustapha, V. Heljanko, V. Johansson, O. Thakali, S. K. Mishra, K. M. Lehto, A. Lipponen, S. Oikarinen, T. Pitkänen, WastPan Study Group and A. Heikinheimo, Wastewater surveillance of antibiotic-resistant bacterial pathogens: a systematic review, *Front. Microbiol.*, 2022, **13**, 977106.

18 F. Zhao, Q. Yu and X.-X. Zhang, A Mini-Review of Antibiotic Resistance Drivers in Urban Wastewater Treatment Plants: Environmental Concentrations, Mechanism and Perspectives, *Water*, 2023, **15**, 3165–3179.

19 M. S. de Ilurdoz, J. J. Sadhwani and J. V. Reboso, Antibiotic removal processes from water & wastewater for the protection of the aquatic environment - a review, *J. Water Process Eng.*, 2022, **45**, 102474.

20 A. Huang, M. Yan, J. Lin, L. Xu, H. Gong and H. Gong, A Review of Processes for Removing Antibiotics from Breeding Wastewater, *Int. J. Environ. Res. Public Health*, 2021, **18**, 4909–4920.

21 V. V. Emzhina, E. N. Kuzin, E. S. Babusenko and N. E. Krutchinina, Photodegradation of tetracycline in presence of H_2O_2 and metal oxide based catalysts, *J. Water Process Eng.*, 2021, **39**, 101696.

22 T. Luo, H. Feng, L. Tang, Y. Lu, W. Tang, S. Chen, J. Yu, Q. Xie, X. Quyang and Z. Chen, Efficient degradation of tetracycline by heterogeneous electro-Fenton process using Cu-doped Fe@Fe_2O_3: Mechanism and degradation pathway, *J. Chem. Eng.*, 2020, **382**, 122970.

23 J. Jiao, Y. Li, Q. Song, L. Wang, T. Luo, C. Gao, L. Liu and S. Yang, Removal of Pharmaceuticals and Personal Care Products (PPCPs) by Free Radicals in Advanced Oxidation Processes, *Materials*, 2022, **15**, 8152–8175.

24 D. Kanakaraju, B. D. Glass and M. Oelgemöller, Advanced oxidation process-mediated removal of pharmaceuticals from water: a review, *J. Environ. Manag.*, 2018, **219**, 189–207.

25 P. Loganathan, S. Vigneswaran, J. Kandasamy, A. K. Cuprys, Z. Maletskyi and H. Ratnaweera, Treatment Trends and Combined Methods in Removing Pharmaceuticals and Personal Care Products from Wastewater—a review, *Membranes*, 2023, **13**, 158–176.

26 K. Ng, N. A. Alygizakis, N. S. Thomaidis and J. Slobodnik, Wide-Scope Target and Suspect Screening of Antibiotics in Effluent Wastewater from Wastewater Treatment Plants in Europe, *Antibiotics*, 2023, **12**, 100–111.

27 S. V. P. Mylapilli and S. N. Reddy, Sub and supercritical water oxidation of pharmaceutical wastewater, *J. Environ. Chem. Eng.*, 2019, **7**, 103165.

28 J. Wang and S. Wang, Removal of pharmaceuticals and personal care products (PPCPs) from wastewater: a review, *J. Environ. Manag.*, 2016, **182**, 620–640.

29 M. Fakioglu, L. Ahrens and I. Ozturk, A Review on Pharmaceuticals Removal from Wastewater Effluents by Single and Combined Ozone-Sorption Systems and Fate of Transformation Products, *Ozone: Sci. Eng.*, 2024, **46**(4), 324–344.

30 P. Kovalakova, L. Cizmas, M. Feng, Th. J. McDonald, B. Marsalek and V. K. Sharma, Oxidation of antibiotics by ferrate(VI) in water: Evaluation of their removal efficiency and toxicity changes, *Chemosphere*, 2021, **277**, 130365.

31 L. Wang, S. Lv, X. Wang, B. Liu and Z. Wang, Ferrate (VI) Oxidation Is an Effective and Safe Way to Degrade Residual Colistin - a Last Resort Antibiotic - in Wastewater, *Front. Vet. Sci.*, 2021, **8**, 773089.

32 B.-J. Ni, X. Yan, X. Dai, Z. Liu, W. Wei, Sh.-L. Wu, Q. Xu and J. Sun, Ferrate effectively removes antibiotic resistance genes from wastewater through combined effect of microbial DNA damage and coagulation, *Water Res.*, 2020, **185**, 116273.

Open Access Article. Published on 25 June 2025. Downloaded on 12/7/2025 12:10:05 AM. This article is licensed under a Creative Commons Attribution-NonCommercial 3.0 Unported Licence.

33 E. Kuzin, Yu. Averina, A. Kurbatov, N. Kruchinina and V. Boldyrev, Titanium-Containing Coagulants in Wastewater Treatment Processes in the Alcohol Industry, *Processes*, 2022, **10**, 440–448.
34 Z. Jiang, Y. Li, S. Wang, C. Cui, C. Yang and J. Li, Review on Mechanisms and Kinetics for Supercritical Water Oxidation Processes, *Appl. Sci.*, 2020, **10**, 4937–4978.
35 M. D. Bermejo and M. J. Cocero, Supercritical water oxidation: A technical review, *AIChE J.*, 2006, **52**, 3933–3951.
36 C. Trellu, B. P. Chaplin, C. Coetsier, R. Esmilaire, S. Cerneaux, C. Causserand and M. Cretin, Electro-oxidation of organic pollutants by reactive electrochemical membranes, *Chemosphere*, 2018, **208**, 159–175.
37 S. V. da Silva, J. B. Welter, L. L. Albornoz, A. N. A. Heberle, J. Z. Ferreira and A. M. Bernandes, Advanced Electrochemical Oxidation Processes in the Treatment of Pharmaceutical Containing Water and Wastewater: a Review, *Curr. Pollut. Rep.*, 2021, **7**, 146–159.
38 R. Fu, P.-S. Zhang, Y.-X. Jiang, L. Sun and X.-H. Sun, Wastewater treatment by anodic oxidation in electrochemical advanced oxidation process: Advance in mechanism, direct and indirect oxidation detection methods, *Chemosphere*, 2023, **311**, 136993.
39 Y. Jiang, H. Zhao, J. Liang, L. Yue, T. Li, Y. Luo, Q. Liu, S. Lu, A. M. Asiri, Z. Gong and X. Sun, Anodic oxidation for the degradation of organic pollutants: Anode materials, operating conditions and mechanisms. A mini review, *Electrochem. Commun.*, 2021, **123**, 106912.
40 M. A. Kabanov, N. A. Ivantsova, E. N. Kuzin, E. D. Murzina and A. Yu. Korobov, Evaluation of the influence of drug complex formation on the efficiency of water conditioning with reagents for tetracycline, *Pharm. Chem. J.*, 2022, **55**, 1245–1249.
41 T. H. Grossman, Tetracycline Antibiotics and Resistance, *Cold Spring Harbor Perspect. Med.*, 2016, **6**, a025387.
42 I. Yahiaoui, F. Aissani-Benissad, F. Fourcade and A. Amrane, Removal of tetracycline hydrochloride from water based on direct anodic oxidation (Pb/PbO_2 electrode) coupled to activated sludge culture, *J. Chem. Eng.*, 2013, **221**, 418–425.
43 W. Yang, J. Tan, Y. Chena, Zh. Li, F. Liu, H. Long, Q. Wei, L. Liu, L. Ma, K. Zhou and Zh. Yu, Relationship between substrate type and BDD electrode structure, performance and antibiotic tetracycline mineralization, *J. Alloys Compd.*, 2021, **890**, 161760.
44 J. Wu, H. Zhang, N. Oturan, Y. Wang, L. Chen and M. A. Oturan, Application of response surface methodology to the removal of the antibiotic tetracycline by electrochemical process using carbon-felt cathode and DSA ($Ti/RuO_2–IrO_2$) anode, *Chemosphere*, 2012, **87**, 614–620.
45 I. Y. Köktas, Ö. Gökkus, I. A. Kariper and A. Otmani, Tetracycline removal from aqueous solution by electrooxidation using ruthenium-coated graphite anode, *Chemosphere*, 2023, **315**, 137758.
46 S. Liang, H. Lin, X. Yan and Q. Huang, Electro-oxidation of Tetracycline by a Magnéli Phase Ti_4O_7 Porous Anode: Kinetics, Products, and Toxicity, *J. Chem. Eng.*, 2017, **332**, 628–636.
47 S. Belkacem, S. Bouafia and M. Chabani, Study of oxytetracycline degradation by means of anodic oxidation process using platinized titanium (Ti/Pt) anode and modeling by artificial neural networks, *Process Saf. Environ. Prot.*, 2017, **111**, 170–179.
48 **https://www.yunchtitanium.com/high-quality-platinum-coated-titanium-anode**.
49 J. Wang, D. Zhi, H. Zhou, X. He and D. Zhang, Evaluating tetracycline degradation pathway and intermediate toxicity during the electrochemical oxidation over a Ti/Ti_4O_7 anode, *Water Res.*, 2018, **137**, 324–334.
50 L. Wang, Y. Wang, Y. Sui, J. Lu, B. Hu and H. Qingguo, Formation of chlorate and perchlorate during electrochemical oxidation by Magnéli phase Ti_4O_7 anode: inhibitory effects of coexisting constituents, *Sci. Rep.*, 2022, **12**, 15880.
51 Zh. Li, Y. Mu, Q. Zhang, H. Huang, X. Wei, L. Yang, G. Wang, T. Zhao, G. Wu and L. Zeng, Constructing highly durable reversal-tolerant anodes *via* integrating high-surface-area Ti_4O_7 supported Pt and $Ir@IrO_x$ for proton exchange membrane fuel cells, *Energy Environ. Sci.*, 2024, **17**, 1580–1591.
52 N. A. Ivantsova, Photooxidative Degradation of Formaldehyde in Aqueous Medium, *High Energy Chem.*, 2021, **55**, 212–215.
53 M. Łukaszewski, M. Soszko and A. Czerwiński, Electrochemical methods of real surface frea determination of noble metal electrodes – an overview, *Int. J. Electrochem. Sci.*, 2016, **11**, 4442–4469.
54 T. Vidaković, M. Christov and K. Sundmacher, The use of CO stripping for *in situ* fuel cell catalyst characterization, *Electrochim. Acta*, 2007, **52**, 5606–5613.
55 Y. Zhu, B. Li, Y. Wang and T. Wang, Preparation of Porous $Ti/RuO_2–IrO_2@Pt$, $Ti/RuO_2–TiO_2@Pt$ and $Ti/Y_2O_3–RuO_2–TiO_2@Pt$ Anodes for Efficient Electrocatalytic Decomposition of Tetracycline, *Catalysis*, 2023, **28**, 2189–2203.
56 T. Bejerano, Ch. Forgacs and E. Gileadi, Selective inhibition of electrode reactions by organic compounds: I. The inhibition of Br_2 and I_2 evolution on platinum by phenol, *J. Electroanal. Chem. Interfacial Electrochem.*, 1970, **27**, 69–79.
57 L. V. Belovolova, Reactive oxygen species in aqueous media (review), *Opt. Spectrosc.*, 2020, **128**, 923–942.
58 P. K. Malik and S. K. Sanyal, Kinetics of decolourisation of azo dyes in wastewater by UV/H_2O_2 process, *Sep. Purif. Technol.*, 2004, **36**, 167–175.
59 R. T. P. Sant'Anna, S. M. P. Santos, G. P. Silva, R. J. R. Ferreira, A. P. Oliveira, C. E. S. Côrtes and R. B. Faria, Kinetics and Mechanism of Chlorate-Chloride Reaction, *J. Braz. Chem. Soc.*, 2012, **23**, 1543–1550.
60 J. F. E. Gootzen, A. H. Wonders, W. Visscher and J. A. R. van Veen, Adsorption of C_3 Alcohols, 1-Butanol, and Ethene on Platinized Platinum As Studied with FTIRS and DEMS, *Langmuir*, 1997, **13**, 1659–1667.
61 J. L. Rodríguez, R. M. Souto, L. Fernández-Mérida and E. Pastor, Revealing Structural Effects: Electrochemical

© 2025 The Author(s). Published by the Royal Society of Chemistry

Open Access Article. Published on 25 June 2025. Downloaded on 12/7/2025 12:10:05 AM.
This article is licensed under a Creative Commons Attribution-NonCommercial 3.0 Unported Licence.

Reactions of Butanols on Platinum, *Chem.–Eur. J.*, 2002, **8**, 2134–2142.

62 A. M. Kamel, H. G. Fouda, P. R. Brown and B. Munson, Mass Spectrum Characterization of Tetracyclines by Electrospray Ionization, H/D Exchange, and Multiple Stage Mass Spectrometry, *J. Am. Soc. Mass Spectrom.*, 2002, **13**, 543–557.

63 P. Kumar, Pharmacology of Specific Drug Groups: Antibiotic Therapy, in *Pharmacology and Therapeutics for Dentistry*, Elsevier, Amsterdam, 7th edn, 2017, pp. 457–487, DOI: **10.1016/B978-0-323-39307-2.00033-3**.

64 F. Carnevale Neto, V. Pascua and D. Raftery, Formation of sodium cluster ions Complicates LC-MS metabolomics analyses, *Rapid Commun. Mass Spectrom.*, 2021, **35**, e9175.

65 **https://sitem.herts.ac.uk/aeru/ppdb/en/Reports/359.htm**.

66 **https://www.nj.gov/dep/watersupply/pdf/append-b-section-i.pdf**.

67 M. Salman, M. Athar, U. Shafique, R. Rehman, S. Ameer, S. Z. Ali and M. Azeem, Removal of formaldehyde from aqueous solution by adsorption on kaolin and bentonite: a comparative study, *Turkish J. Eng. Env. Sci.*, 2012, **36**, 263–270.

68 N. A. Ivantsova, V. V. Kuznetsov, V. I. Tikhonova and A. A. Churina, Removal of Antimicrobial and Analgesic Drugs from Water *via* Electro- and Photo-Oxidation, *Russ. J. Gen. Chem.*, 2024, **94**, 1–5.